Physics Letters B 708 (2012) 265–275

Contents lists available at SciVerse ScienceDirect

Physics Letters B

www.elsevier.com/locate/physletb

Heavy flavour decay muon production at forward rapidity in proton–proton collisions at $\sqrt{s} = 7$ TeV ☆

ALICE Collaboration

ARTICLE INFO

Article history:
Received 20 January 2012
Accepted 24 January 2012
Available online 28 January 2012
Editor: L. Rolandi

Keywords:
LHC
ALICE experiment
pp collisions
Single muons
Heavy flavour production

ABSTRACT

The production of muons from heavy flavour decays is measured at forward rapidity in proton–proton collisions at $\sqrt{s} = 7$ TeV collected with the ALICE experiment at the LHC. The analysis is carried out on a data sample corresponding to an integrated luminosity $L_{\text{int}} = 16.5\ \text{nb}^{-1}$. The transverse momentum and rapidity differential production cross sections of muons from heavy flavour decays are measured in the rapidity range $2.5 < y < 4$, over the transverse momentum range $2 < p_{\text{t}} < 12$ GeV/c. The results are compared to predictions based on perturbative QCD calculations.

1. Introduction

The study of heavy flavour (charm and beauty) production in proton–proton collisions at LHC (Large Hadron Collider) energies provides an important test of perturbative QCD (pQCD) calculations [1,2] in a new energy domain, where unprecedented small Bjorken-x (momentum fraction) values are probed. In the rapidity region $2.5 < y < 4$, charm (beauty) production at $\sqrt{s} = 7$ TeV is expected to be sensitive to x values down to about $6 \cdot 10^{-6}$ ($2 \cdot 10^{-5}$). Important progress has been achieved in the understanding of heavy flavour production at lower energies. In earlier measurements, the beauty production cross section in $\text{p}\bar{\text{p}}$ collisions at $\sqrt{s} = 1.8$ TeV measured by the CDF and D0 experiments [3,4] at the FNAL Tevatron, was found to be higher than Next-to-Leading Order (NLO) pQCD predictions [1]. More recent results from the CDF Collaboration [5], for $\text{p}\bar{\text{p}}$ collisions at $\sqrt{s} = 1.96$ TeV, are described well by Fixed Order Next-to-Leading Log (FONLL) [6,7] and NLO [8] pQCD calculations. The charm production cross section measured at the FNAL Tevatron [9] is also well reproduced by FONLL [10] and GM-VFN [11] calculations within experimental and theoretical uncertainties, although at the upper limit of the calculations. The PHENIX and STAR Collaborations [12,13] at the RHIC (Relativistic Heavy Ion Collider) measured the production of muons and electrons from heavy flavour decays in pp collisions at $\sqrt{s} = 0.2$ TeV. The upper limit of FONLL pQCD calculations [14] is consistent with the measurement of electrons from heavy flavour decays in the mid-rapidity region, while in the forward rapidity region the production of muons from heavy flavour decays is underestimated by the model calculations. Furthermore, at LHC energies, the ATLAS [15], LHCb [16] and CMS [17,18] Collaborations reported on the measurement of beauty production in pp collisions at $\sqrt{s} = 7$ TeV. The results are consistent with NLO pQCD calculations within uncertainties. A similar agreement with FONLL calculations is also observed for mid-rapidity electrons and muons from heavy flavour decays, measured by the ATLAS experiment [19] in pp collisions at $\sqrt{s} = 7$ TeV. In this respect, it is particularly interesting to perform the measurement of heavy flavour decay muon production in the forward rapidity region at the LHC and compare it with theoretical models.

The investigation of heavy flavour production in pp collisions also constitutes an essential baseline for the corresponding measurements in heavy ion collisions. In the latter, heavy quarks are produced at early stages of the collision and then experience the full evolution of the extremely hot and dense, strongly interacting medium [20,21]. The modification of the heavy flavour transverse momentum distributions measured in heavy ion collisions with respect to those measured in pp collisions is considered as a sensitive probe of this medium [22,23].

Finally, the study of heavy flavour production is also important for the understanding of quarkonium production, both in pp, p–nucleus and nucleus–nucleus collisions [20,21].

The ALICE experiment [24] measures the heavy flavour production at mid-rapidity through the semi-electronic decay channel [25] and in a more direct way through the hadronic D-meson decay channel [26], and at forward rapidity through the semi-muonic decay channel. In this Letter, we present the measurement of differential production cross sections of muons from heavy flavour decays in the rapidity range $2.5 < y < 4$ and transverse momentum range $2 < p_{\text{t}} < 12$ GeV/c, with the ALICE muon

---

☆ © CERN for the benefit of the ALICE Collaboration.

0370-2693 © 2012 CERN. Published by Elsevier B.V. Open access under CC BY-NC-ND license.
doi:10.1016/j.physletb.2012.01.063

spectrometer [24], in pp collisions at $\sqrt{s} = 7$ TeV. The results are compared to FONLL pQCD calculations [2,27].

The Letter is organized as follows. Section 2 consists of an overview of the ALICE experiment with an emphasis on the muon spectrometer and a description of data taking conditions. Section 3 is devoted to the analysis strategy: event and track selection, background subtraction, corrections, normalization and determination of systematic uncertainties. Section 4 addresses the experimental results: p_t- and y-differential production cross sections of muons from heavy flavour decays at forward rapidity, and comparisons to FONLL pQCD predictions. Conclusions are given in Section 5.

2. The ALICE experiment and data taking conditions

A detailed description of the ALICE detector can be found in [24]. The apparatus consists of two main parts: a central barrel (pseudo-rapidity coverage: $|\eta| < 0.9$) placed in a large solenoidal magnet ($B = 0.5$ T), which measures hadrons, electrons and photons, and a muon spectrometer ($-4 < \eta < -2.5$[1]). Several smaller detectors for global event characterization and triggering are located in the forward and backward pseudo-rapidity regions. Amongst those, the VZERO detector is used for triggering purposes and in the offline rejection of beam-induced background events. It is composed of two scintillator arrays placed at each side of the interaction point and covering $2.8 < \eta < 5.1$ and $-3.7 < \eta < -1.7$. The central barrel detector used in this work for the interaction vertex measurement is the Silicon Pixel Detector (SPD), the innermost part of the Inner Tracking System (ITS). The SPD consists of two cylindrical layers of silicon pixels covering $|\eta| < 2.0$ and $|\eta| < 1.4$ for the inner and outer layer, respectively. The SPD is also used in the trigger logic.

The muon spectrometer detects muons with momentum larger than 4 GeV/c and is composed of two absorbers, a dipole magnet providing a field integral of 3 Tm, and tracking and trigger chambers. A passive front absorber of 10 interaction lengths (λ_I), made of carbon, concrete and steel, is designed to reduce the contribution of hadrons, photons, electrons and muons from light hadron decays. A small angle beam shield ($\theta < 2°$), made of tungsten, lead and steel, protects the muon spectrometer against secondary particles produced by the interaction of large-η primary particles in the beam pipe. Tracking is performed by means of five tracking stations, each composed of two planes of Cathode Pad Chambers. Stations 1 and 2 (4 and 5) are located upstream (downstream) of the dipole magnet, while station 3 is embedded inside the dipole magnet. The intrinsic spatial resolution of the tracking chambers is better than 100 μm. Two stations of trigger chambers equipped with two planes of Resistive Plate Chambers each are located downstream of the tracking system, behind a 1.2 m thick iron wall of 7.2 λ_I. The latter absorbs most of the hadrons that punch through the front absorber, secondary hadrons produced inside the front absorber and escaping it and low momentum muons ($p < 4$ GeV/c). The spatial resolution of the trigger chambers is better than 1 cm and the time resolution is about 2 ns. Details concerning track reconstruction can be found in [28,29].

The results presented in this publication are based on the analysis of a sample of pp collisions at $\sqrt{s} = 7$ TeV collected in 2010, corresponding to an integrated luminosity of 16.5 nb^{-1}.

The data sample consists of minimum bias trigger events (MB) and muon trigger events (μ-MB), the latter requiring, in addition to the MB trigger conditions, the presence of one muon above a transverse momentum (p_t) threshold that reaches the muon trigger system. The MB trigger is defined as a logical OR between the requirement of at least one hit in the SPD and a hit in one of the two VZERO scintillator arrays. It also asks for a coincidence between the signals from the two beam counters, one on each side of the interaction point, indicating the passage of bunches. This corresponds to at least one charged particle in 8 units of pseudo-rapidity. The logic of the μ-MB trigger requires hits in at least three (out of four possible) trigger chamber planes. The estimate of the muon transverse momentum is based on the deviation of the measured track with respect to a straight line coming from the interaction point, in the bending plane (plane measuring the position along the direction perpendicular to the magnetic field). By applying a cut on this deviation, tracks above a given p_t threshold are selected. The p_t threshold allows the rejection of soft background muons mainly coming from pion and kaon decays, and also to limit the muon trigger rate when high luminosities are delivered at the interaction point. In the considered data taking period, the p_t trigger threshold was set to its minimum value of about 0.5 GeV/c and the corresponding muon trigger rate varied between about 40 and 150 Hz. The instantaneous luminosity at the ALICE interaction point was limited to $0.6\text{–}1.2 \cdot 10^{29}\ \text{cm}^{-2}\,\text{s}^{-1}$ by displacing the beams in the transverse plane by 3.8 times the r.m.s. of their transverse profile. In this way, the probability to have multiple MB interactions in the same bunch crossing is kept below 2.5%.

The alignment of the tracking chambers, a crucial step for the single muon analysis, was carried out using the MILLEPEDE package [30], by analyzing tracks without magnetic field in the dipole and solenoidal magnet. The corresponding resolution is about 300 μm in the bending plane, for tracks with $p_t > 2$ GeV/c. With such alignment precision, the relative momentum resolution of reconstructed tracks ranges between about 1% at a momentum of 20 GeV/c and 4% at 100 GeV/c.

3. Data analysis

The single muon analysis was carried out with muon trigger events while, as will be discussed in Section 3.4, minimum bias trigger events were used to convert differential muon yields into differential cross sections. The identification of muons from charm and beauty decays in the forward region is based on the p_t distribution of reconstructed tracks. Three main background contributions must be subtracted and/or rejected:

- decay muons: muons from the decay of primary light hadrons including pions and kaons (the main contribution) and other meson and baryon decays (such as J/ψ and low mass resonances η, ρ, ω and ϕ);
- secondary muons: muons from secondary light hadron decays produced inside the front absorber;
- punch-through hadrons and secondary hadrons escaping the front absorber and crossing the tracking chambers, which are wrongly reconstructed as muons.

A Monte Carlo simulation based on the GEANT3 transport code [31,32] and using the PYTHIA 6.4.21 event generator [33,34] (tune Perugia-0 [35]) was performed to obtain the p_t distributions of these different contributions. They are displayed in Fig. 1 after all the selection cuts discussed in Section 3.1 were applied. After cuts, the component of muons from heavy flavour decays prevails over the background contribution for $p_t \gtrsim 4$ GeV/c. The simulation results indicate that the hadronic background and the contribution of fake tracks (tracks which are not associated to one single particle crossing the whole spectrometer) are negligible. The component of

---

[1] The muon spectrometer covers a negative pseudo-rapidity range in the ALICE reference frame. η and y variables are identical for muons in the acceptance of the muon spectrometer, and in pp collisions the physics results are symmetric with respect to η $(y) = 0$. They will be presented as a function of y, with positive values.

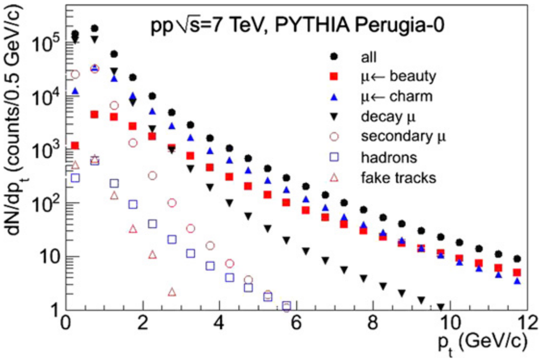

Fig. 1. Transverse momentum distribution of reconstructed tracks in the muon spectrometer after all selection cuts were applied (see Section 3.1 for details). The distributions were obtained from a PYTHIA [33,34] (tune Perugia-0 [35]) simulation of pp collisions at $\sqrt{s} = 7$ TeV. The main sources are indicated in the figure.

muons from $W^{\pm}$ and Z^0 decays, which dominates in the p_t range 30–40 GeV/c [36,19], is not considered in this analysis. This contribution is negligible in the p_t range of interest 2–12 GeV/c.

3.1. Data sample: event and track selection

The data sample used in the physics analysis amounts to $1.3 \cdot 10^7$ μ-MB trigger events. These selected events satisfied the quality criteria on detector conditions during data taking and the analysis quality criteria, which reduced the beam-induced background. This was achieved by using the timing information from the VZERO and by exploiting the correlation between the number of hits and track segments in the SPD. The accepted events have at least one interaction vertex reconstructed from hits correlation in the two SPD layers. The corresponding total number of tracks reconstructed in the muon spectrometer is $7.8 \cdot 10^6$. Various selection cuts were applied in order to reduce the background contributions in the data sample. Tracks were required to be reconstructed in the geometrical acceptance of the muon spectrometer, with $-4 < \eta < -2.5$ and $171° < \theta_{\text{abs}} < 178°$, θ_{abs} being the track polar angle measured at the end of the absorber. These two cuts reject about 9% of tracks. Then, the track candidate measured in the muon tracking chambers was required to be matched with the corresponding one measured in the trigger chambers. This results in a very effective rejection of the hadronic component that is absorbed in the iron wall. This condition is fulfilled for a large fraction of reconstructed tracks since the analysis concerns μ-MB trigger events. The fraction of reconstructed tracks that are not matched with a corresponding one in the trigger system is about 5%. For comparison, in MB collisions this fraction is about 64%. Furthermore, the correlation between momentum and Distance of Closest Approach (DCA, distance between the extrapolated muon track and the interaction vertex, in the plane perpendicular to the beam direction and containing the vertex) was used to remove remaining beam-induced background tracks which do not point to the interaction vertex. Indeed, due to the multiple scattering in the front absorber, the DCA distribution of tracks coming from the interaction vertex is expected to be described by a Gaussian function whose width depends on the absorber material and is proportional to $1/p$. The beam-induced background does not follow this trend and can be rejected by applying a cut on $p \times$ DCA at 5σ, where σ is extracted from a Gaussian fit to the $p \times$ DCA distribution measured in two regions in θ_{abs}, corresponding to different materials in the front absorber. This cut removes 0.4% of tracks, mainly located in the high p_t range (in the region $p_t > 4$ GeV/c, this condition rejects about 13% of tracks). After these cuts, the data sample consists of $6.67 \cdot 10^6$ muon candidates.

The measurement of the heavy flavour decay muon production is performed in the region $p_t > 2$ GeV/c where the contribution of secondary muons is expected to be small (about 3% of the total muon yield, see Fig. 1). In such a p_t region the main background component consists of decay muons and amounts to about 25% of the total yield (see Fig. 1).

3.2. Subtraction of the background contribution of decay muons

The subtraction of the background component from decay muons (muons from primary pion and kaon decays, mainly) is based on simulations, using PYTHIA 6.4.21 [33,34] (tune Perugia-0 [35]) and PHOJET 1.12 [37] as event generators. In order to avoid fluctuations due to the lack of statistics in the high p_t region in the Monte Carlo generators, the reconstructed p_t distribution of decay muons, obtained after all selection cuts are applied (Section 3.1), is fitted using

$$\frac{\mathrm{d}N}{\mathrm{d}p_{\mathrm{t}}}^{\mu\leftarrow\text{decay}} = \frac{\mathrm{a}}{(p_{\mathrm{t}}^2 + \mathrm{b})^{\mathrm{c}}}, \qquad (1)$$

where a, b and c are free parameters. The fits are performed in five rapidity intervals, in the region $2.5 < y < 4$. The normalization is done assuming that the fraction of decay muons in the data is the same as the one in the simulations, in the region where this component is dominant ($p_t < 1$ GeV/c). Finally, the (fitted) p_t distribution is subtracted from the measured muon p_t distribution. The subtracted p_t distribution is the mean of the p_t distributions from the PYTHIA and PHOJET event generators.

The total systematic uncertainty due to this procedure includes contributions from the model input and the transport code (GEANT3 [31,32]). The former takes into account the shape and normalization of the p_t distribution of decay muons, and the observed difference in the $K^{\pm}/\pi^{\pm}$ ratio as a function of p_t in the mid-rapidity region [38] between ALICE data and simulations. The results show that both PYTHIA (tune Perugia-0) and PHOJET underestimate this ratio by about 20%. The corresponding uncertainty due to this difference between data and simulations is propagated to the muon yield in the forward rapidity region. The effect of the transport code is estimated by varying the yield of secondary muons within 100% in such a way to provide a conservative estimate of the systematic uncertainty on the secondary particle production in the front absorber. The systematic uncertainty from the model input varies from about 7% to 2% as y increases from 2.5 to 4, independently of p_t, while the one from the transport code depends both on y and p_t and ranges from 4% ($3.7 < y < 4$) to a maximum of 34% ($p_t = 2$ GeV/c and $2.5 < y < 2.8$). The corresponding values of these systematic uncertainties as a function of p_t and y are summarized in Table 1. They are added in quadrature in the following.

3.3. Corrections

The extracted yields of muons from heavy flavour decays are corrected for acceptance, reconstruction and trigger efficiencies by means of a simulation modelling the response of the muon spectrometer. The procedure is based on the generation of a large sample of muons from beauty decays by using a parameterization of NLO pQCD calculations [29]. The tracking efficiency takes into account the status of each electronic channel and the residual mis-alignment of detection elements. The evolution of the tracking efficiency over time is controlled by weighting the response of electronic channels as a function of time. The typical value of muon tracking efficiency is about 93%. The efficiencies of the muon trigger chambers are obtained directly from data [28] and employed in the simulations. The typical value of such efficiencies

Table 1
Systematic uncertainties introduced by the procedure used for the subtraction of decay muons. MC and transport refer to the systematic uncertainty due to model input and transport code, respectively. See the text for details.

<table>
<tr><th></th><th>MC</th><th colspan="7">Transport</th></tr>
<tr><th></th><th></th><th colspan="7">p_t (GeV/c)</th></tr>
<tr><th></th><th></th><th>[2.0; 2.5]</th><th>[2.5; 3.0]</th><th>[3.0; 3.5]</th><th>[3.5; 4.0]</th><th>[4.0; 4.5]</th><th>[4.5; 5.0]</th><th>>5.0</th></tr>
<tr><td>$2.5 < y < 2.8$</td><td>7%</td><td>34%</td><td>22%</td><td>20%</td><td>16%</td><td>12%</td><td>10%</td><td>6%</td></tr>
<tr><td>$2.8 < y < 3.1$</td><td>5.5%</td><td>22%</td><td>18%</td><td>14%</td><td>12%</td><td>10%</td><td>8%</td><td>6%</td></tr>
<tr><td>$3.1 < y < 3.4$</td><td>4.5%</td><td>10%</td><td>9%</td><td>8%</td><td>7%</td><td colspan="3">6%</td></tr>
<tr><td>$3.4 < y < 3.7$</td><td>3.0%</td><td colspan="7">6%</td></tr>
<tr><td>$3.7 < y < 4.0$</td><td>2.0%</td><td colspan="7">4%</td></tr>
</table>

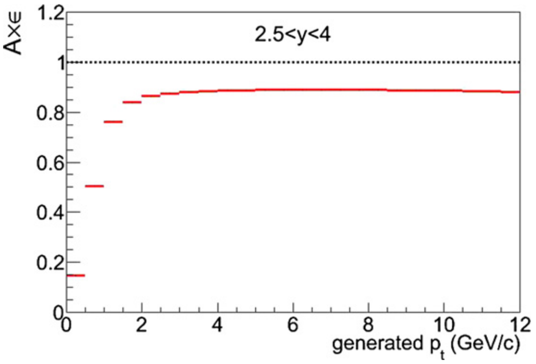

Fig. 2. Acceptance × efficiency as a function of generated p_t, obtained from a simulation of muons from beauty decays.

is about 96%. Fig. 2 shows the resulting acceptance and efficiency ($A \times \varepsilon$) as a function of generated p_t. The global $A \times \varepsilon$ increases significantly up to about 2 GeV/c and tends to saturate at a value close to 90%.

The systematic uncertainty corresponding to the sensitivity of $A \times \varepsilon$ on the input p_t and y distributions was estimated by comparing the results with those from a simulation using muons from charm decays. This amounted to less than 1% and was neglected. The accuracy in the detector modelling introduces a systematic uncertainty estimated to be 5%, by comparing the values of trigger and tracking efficiencies extracted from data and simulations [28].

The distortion of the measured p_t distribution, dominated in the high p_t region by the effect of residual mis-alignment, is also corrected for by introducing in the simulation a residual mis-alignment of the same order of magnitude as in the data. However, this residual mis-alignment is generated randomly. A p_t dependent relative systematic uncertainty on the muon yield of $1\% \times p_t$ (in GeV/c) is considered in order to take into account the differences between the real (unknown) residual mis-alignment and the simulated one. This is a conservative value determined by comparing the reconstructed p_t distribution with or without including the residual mis-alignment.

3.4. Production cross section normalization

The differential production cross section is obtained by normalizing the corrected yields of muons from heavy flavour decays to the integrated luminosity. Since the yields have been extracted using μ-MB trigger events, the differential production cross section is calculated according to

$$\frac{d^2\sigma_{\mu^\pm \leftarrow \mathrm{HF}}}{dp_t\,dy} = \frac{d^2N_{\mu^\pm \leftarrow \mathrm{HF}}}{dp_t\,dy} \times \frac{N^{\mu^\pm}_{\mathrm{MB}}}{N^{\mu^\pm}_{\mu\text{-MB}}} \times \frac{\sigma_{\mathrm{MB}}}{N_{\mathrm{MB}}}, \qquad (2)$$

where:

- $\frac{d^2N_{\mu^\pm \leftarrow \mathrm{HF}}}{dp_t\,dy}$ is the p_t- and y-differential yield of muons from heavy flavour decays;
- $N^{\mu^\pm}_{\mathrm{MB}}$ and $N^{\mu^\pm}_{\mu\text{-MB}}$ are the numbers of reconstructed tracks that satisfy the analysis cuts in MB and μ-MB trigger events, respectively;
- N_{MB} is the number of minimum bias collisions corrected as a function of time by the probability to have multiple MB interactions in a single bunch crossing, and σ_{MB} is the corresponding measured minimum bias cross section.

σ_{MB} is derived from the $\sigma_{\mathrm{VZERO\text{-}AND}}$ cross section [39] measured with the van der Meer scan method [40]. The VZERO-AND condition is defined as a logical AND between signals in the two VZERO scintillator arrays. Such a combination allows one to reduce the sensitivity to beam-induced background. The $\sigma_{\mathrm{VZERO\text{-}AND}}/\sigma_{\mathrm{MB}}$ ratio is the fraction of minimum bias events where the VZERO-AND condition is fulfilled. Its value is 0.87 and it remains stable within 1% over the analyzed data sample. This gives $\sigma_{\mathrm{MB}} = 62.5 \pm 2.2$ (syst.) mb. The statistical uncertainty is negligible, while the 3.5% systematic uncertainty is mainly due to the uncertainty on the beam intensities [41] and on the analysis procedure related to the van der Meer scan of the VZERO-AND signal. Other effects, such as oscillation in the ratio between MB and VZERO-AND counts, contribute less than 1%.

3.5. Summary of systematic uncertainties

The systematic uncertainty on the measurements of the p_t- and y-differential production cross sections of muons from heavy flavour decays accounts for the following contributions discussed in the previous sections:

- background subtraction: from about 5% ($3.7 < y < 4$) to a maximum of 35% ($2.5 < y < 2.8$, $p_t = 2$ GeV/c), see Section 3.2 and Table 1;
- detector response: 5% (Section 3.3);
- residual mis-alignment: $1\% \times p_t$ (Section 3.3);
- luminosity measurement: 3.5% (Section 3.4).

The resulting systematic uncertainty, in the rapidity region $2.5 < y < 4$, varies between 8–14% (the 3.5% systematic uncertainty on the normalization is not included).

4. Results and model comparisons

The measured differential production cross sections of muons from heavy flavour decays as a function of p_t in the rapidity region $2.5 < y < 4$ and as a function of y in the range $2 < p_t < 12$ GeV/c are displayed in Fig. 3 (circles), left and right panels, respectively. The error bars (which are smaller than symbols in most of the p_t and y bins) represent the statistical uncertainties. The boxes correspond to the systematic uncertainties. The

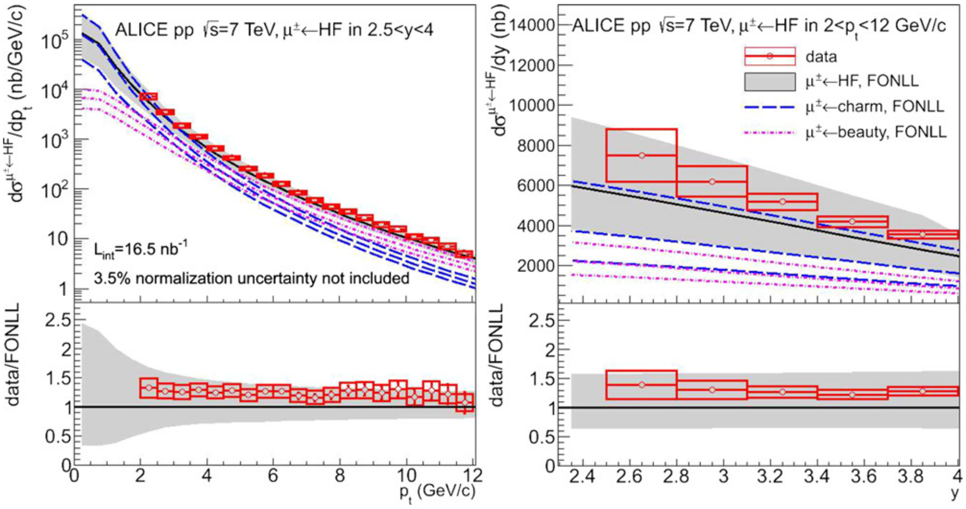

Fig. 3. Left: p_t-differential production cross section of muons from heavy flavour decays in the rapidity range $2.5 < y < 4$. Right: y-differential production cross section of muons from heavy flavour decays, in the range $2 < p_t < 12$ GeV/c. In both panels, the error bars (empty boxes) represent the statistical (systematic) uncertainties. A 3.5% normalization uncertainty is not shown. The solid curves are FONLL calculations and the bands display the theoretical systematic uncertainties. Also shown, are the FONLL calculations and systematic theoretical uncertainties for muons from charm (long dashed curves) and beauty (dashed curves) decays. The lower panels show the corresponding ratios between data and FONLL calculations.

systematic uncertainty on σ_{MB} is not included in the boxes. The results are compared to FONLL predictions [2,27] (black curve and shaded band for the systematic uncertainty). The central values of FONLL calculations use CTEQ6.6 [42] parton distribution functions, a charm quark mass (m_c) of 1.5 GeV/c^2, a beauty quark mass (m_b) of 4.75 GeV/c^2 and the renormalization (μ_R) and factorization (μ_F) QCD scales such that $\mu_R/\mu_0 = \mu_F/\mu_0 = 1$ ($\mu_0 = m_{t,q} = \sqrt{p_t^2 + m_q^2}$). The theoretical uncertainties correspond to the variation of charm and beauty quark masses in the ranges $1.3 < m_c < 1.7$ GeV/c^2 and $4.5 < m_b < 5.0$ GeV/c^2, and QCD scales in the ranges $0.5 < \mu_R/\mu_0 < 2$ and $0.5 < \mu_F/\mu_0 < 2$ with the constraint $0.5 < \mu_F/\mu_R < 2$. The FONLL predictions for muons from beauty decays include the components of muons coming from direct b-hadron decays and from b-hadron decays via c-hadron decays (e.g. $\mathrm{B} \to \mathrm{D} \to \mu$ channel). The uncertainty band is the envelope of the resulting cross sections. The ratios between data and FONLL predictions are shown in the bottom panels. A good description of the data is observed within uncertainties, for both the p_t distribution (up to 12 GeV/c) and the y distribution (in the p_t range from 2 to 12 GeV/c). The measured production cross sections are systematically larger than the central values of the model predictions. The ratio of data over central values of FONLL calculations as a function of p_t and y is about 1.3 over the whole p_t and y ranges. This is consistent with the ALICE measurements of the p_t-differential production cross sections of D mesons [26] in the central rapidity region. The CMS and ATLAS Collaborations made complementary measurements of the heavy flavour production, with electrons and/or muons measured at mid-rapidity in pp collisions at $\sqrt{s} = 7$ TeV [18,19]. The production of muons from beauty decays, measured by the CMS Collaboration in $|\eta| < 2.1$ and at high p_t ($p_t > 6$ GeV/c), exhibits a similar agreement with NLO pQCD calculations within uncertainties: the data points lie in the upper limit of the model predictions. The results from the ATLAS Collaboration concerning the production of muons and electrons from heavy flavour decays in $|\eta| < 2.0$ (excluding $1.37 < |\eta| < 1.52$) and in the region $7 < p_t < 27$ GeV/c are also consistent with FONLL calculations.

The theoretical charm and beauty components are also displayed in Fig. 3. According to these predictions, the muon contribution from beauty decays is expected to dominate in the range $p_t \gtrsim 6$ GeV/c. In this region, it represents about 62% of the heavy flavour decay muon cross section.

A similar comparison between data and FONLL calculations was performed in five rapidity intervals from $y = 2.5$ to $y = 4$ (Fig. 4, upper panels). The corresponding ratio of data over FONLL predictions is depicted in the lower panels of Fig. 4. The model calculations provide an overall good description of the data up to $p_t = 12$ GeV/c in all rapidity intervals, within experimental and theoretical uncertainties.

5. Conclusions

We have presented measurements of the differential production cross sections of muons from heavy flavour decays in the rapidity range $2.5 < y < 4$ and transverse momentum range $2 < p_t < 12$ GeV/c, in pp collisions at $\sqrt{s} = 7$ TeV with the ALICE experiment. The FONLL pQCD calculations are in good agreement with data within experimental and theoretical uncertainties, although the data are close to the upper limit of the model calculations. Both the p_t and y dependence of the heavy flavour decay muon production cross section is well described by the model predictions. The results provide an important baseline for the study of heavy quark medium effects in nucleus–nucleus collisions.

Acknowledgements

The ALICE Collaboration would like to thank all its engineers and technicians for their invaluable contributions to the construction of the experiment and the CERN accelerator teams for the outstanding performance of the LHC complex.

The ALICE Collaboration would like to thank M. Cacciari for providing the pQCD predictions that are compared to these data.

The ALICE Collaboration acknowledges the following funding agencies for their support in building and running the ALICE detector:

Calouste Gulbenkian Foundation from Lisbon and Swiss Fonds Kidagan, Armenia;

Conselho Nacional de Desenvolvimento Científico e Tecnológico (CNPq), Financiadora de Estudos e Projetos (FINEP), Fundação de Amparo à Pesquisa do Estado de São Paulo (FAPESP);

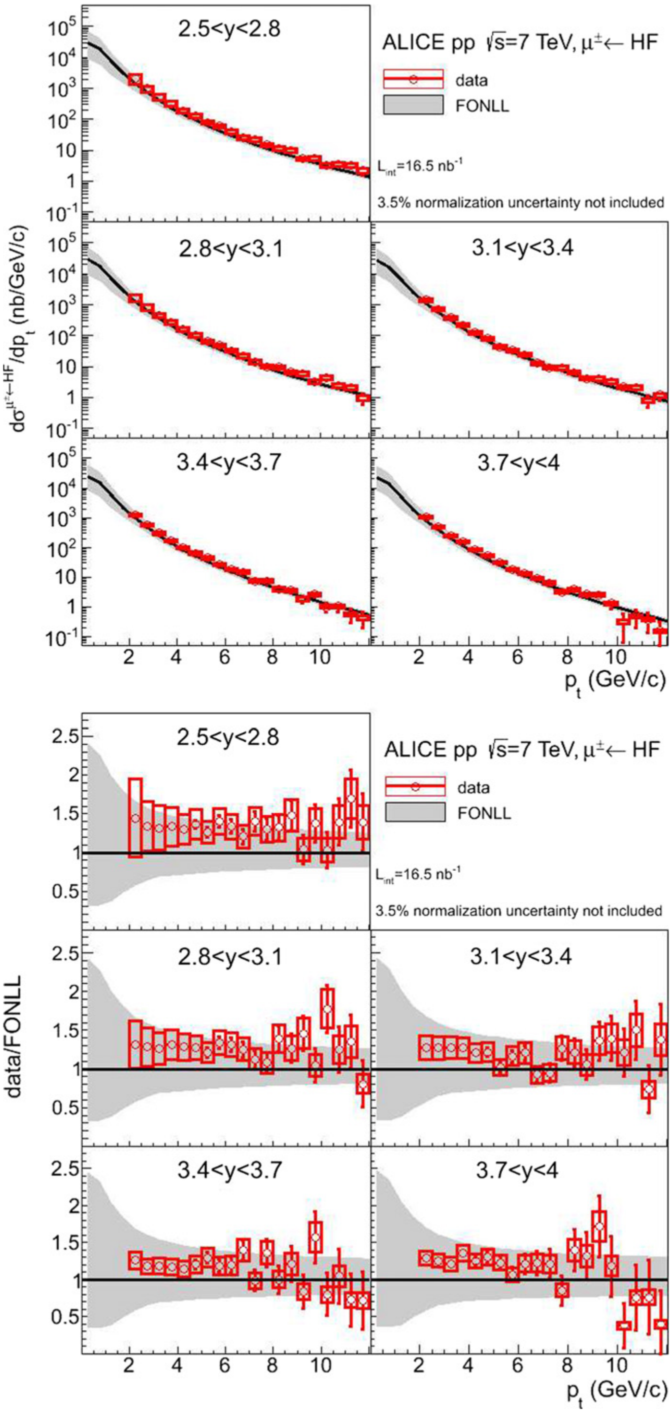

Fig. 4. Upper panel: p_t-differential production cross section of muons from heavy flavour decays in five rapidity regions mentioned in the figures. The error bars (empty boxes) represent the statistical (systematic) uncertainties. A 3.5% normalization uncertainty is not shown. The solid curves are FONLL calculations and the bands display the theoretical systematic uncertainty. Lower panel: ratio between data and FONLL calculations.

National Natural Science Foundation of China (NSFC), the Chinese Ministry of Education (CMOE) and the Ministry of Science and Technology of China (MSTC);

Ministry of Education and Youth of the Czech Republic;

Danish Natural Science Research Council, the Carlsberg Foundation and the Danish National Research Foundation;

The European Research Council under the European Community's Seventh Framework Programme;

Helsinki Institute of Physics and the Academy of Finland;

French CNRS-IN2P3, the 'Region Pays de Loire', 'Region Alsace', 'Region Auvergne' and CEA, France;

German BMBF and the Helmholtz Association;

General Secretariat for Research and Technology, Ministry of Development, Greece;

Hungarian OTKA and National Office for Research and Technology (NKTH);

Department of Atomic Energy and Department of Science and Technology of the Government of India;

Istituto Nazionale di Fisica Nucleare (INFN) of Italy;

MEXT Grant-in-Aid for Specially Promoted Research, Japan;

Joint Institute for Nuclear Research, Dubna;

National Research Foundation of Korea (NRF);

CONACYT, DGAPA, México, ALFA-EC and the HELEN Program (High-Energy physics Latin-American–European Network);

Stichting voor Fundamenteel Onderzoek der Materie (FOM) and the Nederlandse Organisatie voor Wetenschappelijk Onderzoek (NWO), Netherlands;

Research Council of Norway (NFR);

Polish Ministry of Science and Higher Education;

National Authority for Scientific Research – NASR (Autoritatea Naţională pentru Cercetare Ştiinţifică – ANCS);

Federal Agency of Science of the Ministry of Education and Science of Russian Federation, International Science and Technology Center, Russian Academy of Sciences, Russian Federal Agency of Atomic Energy, Russian Federal Agency for Science and Innovations and CERN-INTAS;

Ministry of Education of Slovakia;

Department of Science and Technology, South Africa;

CIEMAT, EELA, Ministerio de Educación y Ciencia of Spain, Xunta de Galicia (Consellería de Educación), CEADEN, Cubaenergía, Cuba, and IAEA (International Atomic Energy Agency);

Swedish Research Council (VR) and Knut & Alice Wallenberg Foundation (KAW);

Ukraine Ministry of Education and Science;

United Kingdom Science and Technology Facilities Council (STFC);

The United States Department of Energy, the United States National Science Foundation, the State of Texas, and the State of Ohio.

Open Access

References

[1] M.L. Mangano, P. Nason, G. Ridolfi, Nucl. Phys. B 373 (1992) 295.
[2] M. Cacciari, M. Greco, P. Nason, JHEP 9805 (1998) 007.
[3] S. Abachi, et al., D0 Collaboration, Phys. Rev. Lett. 74 (1995) 3548;
B. Abbott, et al., D0 Collaboration, Phys. Lett. B 487 (2000) 264;
B. Abbott, et al., D0 Collaboration, Phys. Rev. Lett. 85 (2000) 5068.
[4] F. Abe, et al., CDF Collaboration, Phys. Rev. Lett. 71 (1993) 500;
F. Abe, et al., CDF Collaboration, Phys. Rev. Lett. 71 (1993) 2396;
D. Acosta, et al., CDF Collaboration, Phys. Rev. D 65 (2002) 052005.
[5] D. Acosta, et al., CDF Collaboration, Phys. Rev. D 71 (2005) 032001;
A. Abulencia, et al., CDF Collaboration, Phys. Rev. D 75 (2007) 012010;
T. Aaltonen, et al., CDF Collaboration, Phys. Rev. D 79 (2009) 092003.
[6] M. Cacciari, P. Nason, Phys. Rev. Lett. 89 (2002) 122003.
[7] M. Cacciari, et al., JHEP 0407 (2004) 033.
[8] B.A. Kniehl, et al., Phys. Rev. D 77 (2008) 014011.
[9] D. Acosta, et al., CDF Collaboration, Phys. Rev. Lett. 91 (2003) 241804.
[10] M. Cacciari, P. Nason, JHEP 0309 (2003) 006.
[11] B.A. Kniehl, et al., Phys. Rev. Lett. 96 (2006) 012001.

[12] S.S. Adler, et al., PHENIX Collaboration, Phys. Rev. Lett. 96 (2006) 032001;
A. Adare, et al., PHENIX Collaboration, Phys. Rev. Lett. 97 (2006) 252002;
S.S. Adler, et al., PHENIX Collaboration, Phys. Rev. D 76 (2007) 092002;
A. Adare, et al., PHENIX Collaboration, Phys. Rev. Lett. 103 (2009) 082002.

[13] B.I. Abelev, et al., STAR Collaboration, Phys. Rev. Lett. 98 (2007) 192301;
W. Xie, STAR Collaboration, PoS DIS (2010) 182.

[14] M. Cacciari, P. Nason, R. Vogt, Phys. Rev. Lett. 95 (2005) 122001.

[15] J. Kirk, ATLAS Collaboration, PoS (2010) 013.

[16] R. Aaij, et al., LHCb Collaboration, Phys. Lett. B 694 (2010) 209;
R. Aaij, et al., LHCb Collaboration, Eur. Phys. J. C 71 (2011) 1645.

[17] V. Khachatryan, et al., CMS Collaboration, Phys. Rev. Lett. 106 (2011) 112001;
S. Chatrchyan, et al., CMS Collaboration, Phys. Rev. Lett. 106 (2011) 252001;
P. Bellan, CMS Collaboration, arXiv:1109.2003 [hep-ex].

[18] V. Khachatryan, et al., CMS Collaboration, JHEP 1103 (2011) 090.

[19] G. Aad, et al., ATLAS Collaboration, CERN-PH-EP-2011-108, arXiv:1109.0525 [hep-ex].

[20] F. Carminati, et al., ALICE Collaboration, J. Phys. G: Nucl. Part. Phys. 30 (2004) 1517.

[21] B. Alessandro, et al., ALICE Collaboration, J. Phys. G: Nucl. Part. Phys. 32 (2006) 1295.

[22] N. Armesto, et al., Phys. Rev. D 71 (2005) 050427.

[23] M. Djordjevic, M. Gyulassy, S. Wicks, Phys. Rev. Lett. 94 (2005) 112301;
A.D. Frawley, T. Ullrich, R. Vogt, Phys. Rep. 462 (2008) 125.

[24] K. Aamodt, et al., ALICE Collaboration, JINST 3 (2008) S08002.

[25] A. Dainese, et al., ALICE Collaboration, J. Phys. G: Nucl. Part. Phys. 38 (2011) 124032, and references therein.

[26] B. Abelev, et al., ALICE Collaboration, arXiv:1111.1553 [hep-ex].

[27] M. Cacciari, S. Frixione, N. Houdeau, M.L. Mangano, P. Nason, G. Ridolfi, CERN-PH-TH/2011-227.

[28] K. Aamodt, et al., ALICE Collaboration, Phys. Lett. B 704 (2011) 442.

[29] L. Aphecetche, et al., ALICE Internal Note ALICE-INT-2009-044, https://edms.cern.ch/document/1054937/1.

[30] V. Blobel, C. Kleinwort, arXiv:hep-ex/0208021.

[31] R. Brun, et al., GEANT3 User Guide, CERN, Data Handling Division DD/EE/841, 1985.

[32] R. Brun, et al., CERN Program Library Long Write-up, W5013, GEANT Detector Description and Simulation Tool, 1994.

[33] T. Sjöstrand, Comput. Phys. Commun. 82 (1994) 74.

[34] T. Sjöstrand, S. Mrenna, P. Skands, JHEP 0605 (2006) 026.

[35] P.Z. Skands, Phys. Rev. D 82 (2010) 074018.

[36] Z. Conesa del Valle, et al., ALICE Collaboration, Eur. Phys. J. C 49 (2007) 149.

[37] R. Engel, J. Ranft, S. Roesler, Phys. Rev. D 52 (1995) 1459.

[38] M. Chojnacki, et al., ALICE Collaboration, J. Phys. G: Nucl. Part. Phys. 38 (2011) 124074.

[39] M. Gagliardi, et al., ALICE Collaboration, arXiv:1109.5369 [hep-ex];
B. Abelev, et al., ALICE Collaboration, Measurement of inelastic, single and double diffraction cross sections in proton–proton collisions at LHC with ALICE, in preparation;
L. Aphecetche, et al., ALICE-SCIENTIFIC-NOTE-2011-001.

[40] S. van der Meer, ISR-PO/68-31, KEK68-64.

[41] A. Alici, et al., CERN-ATS-Note-2011-016 PERF.

[42] P.M. Nadolsky, et al., Phys. Rev. D 78 (2008) 013004.

ALICE Collaboration

B. Abelev[69], J. Adam[34], D. Adamová[74], A.M. Adare[120], M.M. Aggarwal[78], G. Aglieri Rinella[30], A.G. Agocs[60], A. Agostinelli[19], S. Aguilar Salazar[56], Z. Ahammed[116], N. Ahmad[14], A. Ahmad Masoodi[14], S.U. Ahn[64,37], A. Akindinov[46], D. Aleksandrov[89], B. Alessandro[95], R. Alfaro Molina[56], A. Alici[96,30,9], A. Alkin[2], E. Almaráz Aviña[56], T. Alt[36], V. Altini[28,30], S. Altinpinar[15], I. Altsybeev[117], C. Andrei[71], A. Andronic[86], V. Anguelov[83], J. Anielski[54], C. Anson[16], T. Antičić[87], F. Antinori[100], P. Antonioli[96], L. Aphecetche[102], H. Appelshäuser[52], N. Arbor[65], S. Arcelli[19], A. Arend[52], N. Armesto[13], R. Arnaldi[95], T. Aronsson[120], I.C. Arsene[86], M. Arslandok[52], A. Asryan[117], A. Augustinus[30], R. Averbeck[86], T.C. Awes[75], J. Äystö[38], M.D. Azmi[14], M. Bach[36], A. Badalà[97], Y.W. Baek[64,37], R. Bailhache[52], R. Bala[95], R. Baldini Ferroli[9], A. Baldisseri[12], A. Baldit[64], F. Baltasar Dos Santos Pedrosa[30], J. Bán[47], R.C. Baral[48], R. Barbera[24], F. Barile[28], G.G. Barnaföldi[60], L.S. Barnby[91], V. Barret[64], J. Bartke[104], M. Basile[19], N. Bastid[64,*], B. Bathen[54], G. Batigne[102], B. Batyunya[59], C. Baumann[52], I.G. Bearden[72], H. Beck[52], I. Belikov[58], F. Bellini[19], R. Bellwied[110], E. Belmont-Moreno[56], G. Bencedi[60], S. Beole[26], I. Berceanu[71], A. Bercuci[71], Y. Berdnikov[76], D. Berenyi[60], C. Bergmann[54], D. Berzano[95], L. Betev[30], A. Bhasin[81], A.K. Bhati[78], L. Bianchi[26], N. Bianchi[66], C. Bianchin[22], J. Bielčík[34], J. Bielčíková[74], A. Bilandzic[73], S. Bjelogrlic[45], F. Blanco[7], F. Blanco[110], D. Blau[89], C. Blume[52], M. Boccioli[30], N. Bock[16], A. Bogdanov[70], H. Bøggild[72], M. Bogolyubsky[43], L. Boldizsár[60], M. Bombara[35], J. Book[52], H. Borel[12], A. Borissov[119], S. Bose[90], F. Bossú[30,26], M. Botje[73], S. Böttger[51], B. Boyer[42], P. Braun-Munzinger[86], M. Bregant[102], T. Breitner[51], T.A. Browning[84], M. Broz[33], R. Brun[30], E. Bruna[120,26,95], G.E. Bruno[28], D. Budnikov[88], H. Buesching[52], S. Bufalino[26,95], K. Bugaiev[2], O. Busch[83], Z. Buthelezi[80], D. Caballero Orduna[120], D. Caffarri[22], X. Cai[40], H. Caines[120], E. Calvo Villar[92], P. Camerini[20], V. Canoa Roman[8,1], G. Cara Romeo[96], W. Carena[30], F. Carena[30], N. Carlin Filho[107], F. Carminati[30], C.A. Carrillo Montoya[30], A. Casanova Díaz[66], M. Caselle[30], J. Castillo Castellanos[12], J.F. Castillo Hernandez[86], E.A.R. Casula[21], V. Catanescu[71], C. Cavicchioli[30], J. Cepila[34], P. Cerello[95], B. Chang[38,123], S. Chapeland[30], J.L. Charvet[12], S. Chattopadhyay[90], S. Chattopadhyay[116], M. Cherney[77], C. Cheshkov[30,109], B. Cheynis[109], E. Chiavassa[95], V. Chibante Barroso[30], D.D. Chinellato[108], P. Chochula[30], M. Chojnacki[45], P. Christakoglou[73,45], C.H. Christensen[72], P. Christiansen[29], T. Chujo[114], S.U. Chung[85], C. Cicalo[93], L. Cifarelli[19,30], F. Cindolo[96], J. Cleymans[80], F. Coccetti[9], J.-P. Coffin[58], F. Colamaria[28], D. Colella[28], G. Conesa Balbastre[65], Z. Conesa del Valle[30,58], P. Constantin[83], G. Contin[20], J.G. Contreras[8], T.M. Cormier[119], Y. Corrales Morales[26], P. Cortese[27], I. Cortés Maldonado[1], M.R. Cosentino[68,108], F. Costa[30], M.E. Cotallo[7], E. Crescio[8], P. Crochet[64], E. Cruz Alaniz[56], E. Cuautle[55], L. Cunqueiro[66], A. Dainese[22,100], H.H. Dalsgaard[72], A. Danu[50], K. Das[90], I. Das[90,42], D. Das[90], A. Dash[48,108], S. Dash[41,95], S. De[116], A. De Azevedo Moregula[66], G.O.V. de Barros[107], A. De Caro[25,9], G. de Cataldo[94],

J. de Cuveland[36], A. De Falco[21], D. De Gruttola[25], H. Delagrange[102], E. Del Castillo Sanchez[30], A. Deloff[101], V. Demanov[88], N. De Marco[95], E. Dénes[60], S. De Pasquale[25], A. Deppman[107], G. D Erasmo[28], R. de Rooij[45], D. Di Bari[28], T. Dietel[54], C. Di Giglio[28], S. Di Liberto[99], A. Di Mauro[30], P. Di Nezza[66], R. Divià[30], Ø. Djuvsland[15], A. Dobrin[119,29], T. Dobrowolski[101], I. Domínguez[55], B. Dönigus[86], O. Dordic[18], O. Driga[102], A.K. Dubey[116], L. Ducroux[109], P. Dupieux[64], A.K. Dutta Majumdar[90], M.R. Dutta Majumdar[116], D. Elia[94], D. Emschermann[54], H. Engel[51], H.A. Erdal[32], B. Espagnon[42], M. Estienne[102], S. Esumi[114], D. Evans[91], G. Eyyubova[18], D. Fabris[22,100], J. Faivre[65], D. Falchieri[19], A. Fantoni[66], M. Fasel[86], R. Fearick[80], A. Fedunov[59], D. Fehlker[15], L. Feldkamp[54], D. Felea[50], G. Feofilov[117], A. Fernández Téllez[1], R. Ferretti[27], A. Ferretti[26], J. Figiel[104], M.A.S. Figueredo[107], S. Filchagin[88], R. Fini[94], D. Finogeev[44], F.M. Fionda[28], E.M. Fiore[28], M. Floris[30], S. Foertsch[80], P. Foka[86], S. Fokin[89], E. Fragiacomo[98], M. Fragkiadakis[79], U. Frankenfeld[86], U. Fuchs[30], C. Furget[65], M. Fusco Girard[25], J.J. Gaardhøje[72], M. Gagliardi[26], A. Gago[92], M. Gallio[26], D.R. Gangadharan[16], P. Ganoti[75], C. Garabatos[86], E. Garcia-Solis[10], I. Garishvili[69], J. Gerhard[36], M. Germain[102], C. Geuna[12], M. Gheata[30], A. Gheata[30], B. Ghidini[28], P. Ghosh[116], P. Gianotti[66], M.R. Girard[118], P. Giubellino[30], E. Gladysz-Dziadus[104], P. Glässel[83], R. Gomez[106], E.G. Ferreiro[13], L.H. González-Trueba[56], P. González-Zamora[7], S. Gorbunov[36], A. Goswami[82], S. Gotovac[103], V. Grabski[56], L.K. Graczykowski[118], R. Grajcarek[83], A. Grelli[45], A. Grigoras[30], C. Grigoras[30], V. Grigoriev[70], S. Grigoryan[59], A. Grigoryan[121], B. Grinyov[2], N. Grion[98], P. Gros[29], J.F. Grosse-Oetringhaus[30], J.-Y. Grossiord[109], R. Grosso[30], F. Guber[44], R. Guernane[65], C. Guerra Gutierrez[92], B. Guerzoni[19], M. Guilbaud[109], K. Gulbrandsen[72], T. Gunji[113], R. Gupta[81], A. Gupta[81], H. Gutbrod[86], Ø. Haaland[15], C. Hadjidakis[42], M. Haiduc[50], H. Hamagaki[113], G. Hamar[60], B.H. Han[17], L.D. Hanratty[91], A. Hansen[72], Z. Harmanova[35], J.W. Harris[120], M. Hartig[52], D. Hasegan[50], D. Hatzifotiadou[96], A. Hayrapetyan[30,121], S.T. Heckel[52], M. Heide[54], H. Helstrup[32], A. Herghelegiu[71], G. Herrera Corral[8], N. Herrmann[83], K.F. Hetland[32], B. Hicks[120], P.T. Hille[120], B. Hippolyte[58], T. Horaguchi[114], Y. Hori[113], P. Hristov[30], I. Hřivnáčová[42], M. Huang[15], S. Huber[86], T.J. Humanic[16], D.S. Hwang[17], R. Ichou[64], R. Ilkaev[88], I. Ilkiv[101], M. Inaba[114], E. Incani[21], P.G. Innocenti[30], G.M. Innocenti[26], M. Ippolitov[89], M. Irfan[14], C. Ivan[86], A. Ivanov[117], V. Ivanov[76], M. Ivanov[86], O. Ivanytskyi[2], A. Jachołkowski[30], P.M. Jacobs[68], L. Jancurová[59], H.J. Jang[63], S. Jangal[58], M.A. Janik[118], R. Janik[33], P.H.S.Y. Jayarathna[110], S. Jena[41], R.T. Jimenez Bustamante[55], L. Jirden[30], P.G. Jones[91], H. Jung[37], W. Jung[37], A. Jusko[91], A.B. Kaidalov[46], V. Kakoyan[121], S. Kalcher[36], P. Kaliňák[47], M. Kalisky[54], T. Kalliokoski[38], A. Kalweit[53], K. Kanaki[15], J.H. Kang[123], V. Kaplin[70], A. Karasu Uysal[30,122], O. Karavichev[44], T. Karavicheva[44], E. Karpechev[44], A. Kazantsev[89], U. Kebschull[62,51], R. Keidel[124], S.A. Khan[116], P. Khan[90], M.M. Khan[14], A. Khanzadeev[76], Y. Kharlov[43], B. Kileng[32], D.J. Kim[38], T. Kim[123], S. Kim[17], S.H. Kim[37], M. Kim[123], J.S. Kim[37], J.H. Kim[17], D.W. Kim[37], B. Kim[123], S. Kirsch[36,30], I. Kisel[36], S. Kiselev[46], A. Kisiel[30,118], J.L. Klay[4], J. Klein[83], C. Klein-Bösing[54], M. Kliemant[52], A. Kluge[30], M.L. Knichel[86], K. Koch[83], M.K. Köhler[86], A. Kolojvari[117], V. Kondratiev[117], N. Kondratyeva[70], A. Konevskikh[44], A. Korneev[88], C. Kottachchi Kankanamge Don[119], R. Kour[91], M. Kowalski[104], S. Kox[65], G. Koyithatta Meethaleveedu[41], J. Kral[38], I. Králik[47], F. Kramer[52], I. Kraus[86], T. Krawutschke[83,31], M. Krelina[34], M. Kretz[36], M. Krivda[91,47], F. Krizek[38], M. Krus[34], E. Kryshen[76], M. Krzewicki[73,86], Y. Kucheriaev[89], C. Kuhn[58], P.G. Kuijer[73], P. Kurashvili[101], A.B. Kurepin[44], A. Kurepin[44], A. Kuryakin[88], S. Kushpil[74], V. Kushpil[74], H. Kvaerno[18], M.J. Kweon[83], Y. Kwon[123], P. Ladrón de Guevara[55], I. Lakomov[42,117], R. Langoy[15], C. Lara[51], A. Lardeux[102], P. La Rocca[24], C. Lazzeroni[91], R. Lea[20], Y. Le Bornec[42], S.C. Lee[37], K.S. Lee[37], F. Lefèvre[102], J. Lehnert[52], L. Leistam[30], M. Lenhardt[102], V. Lenti[94], H. León[56], I. León Monzón[106], H. León Vargas[52], P. Lévai[60], X. Li[11], J. Lien[15], R. Lietava[91], S. Lindal[18], V. Lindenstruth[36], C. Lippmann[86,30], M.A. Lisa[16], L. Liu[15], P.I. Loenne[15], V.R. Loggins[119], V. Loginov[70], S. Lohn[30], D. Lohner[83], C. Loizides[68], K.K. Loo[38], X. Lopez[64], E. López Torres[6], G. Løvhøiden[18], X.-G. Lu[83], P. Luettig[52], M. Lunardon[22], J. Luo[40,64], G. Luparello[45], L. Luquin[102], C. Luzzi[30], R. Ma[120], K. Ma[40], D.M. Madagodahettige-Don[110], A. Maevskaya[44], M. Mager[53,30], D.P. Mahapatra[48], A. Maire[58], M. Malaev[76], I. Maldonado Cervantes[55], L. Malinina[59,i], D. Mal'Kevich[46], P. Malzacher[86], A. Mamonov[88], L. Manceau[95], L. Mangotra[81], V. Manko[89], F. Manso[64], V. Manzari[94], Y. Mao[65,40], M. Marchisone[64,26], J. Mareš[49], G.V. Margagliotti[20,98], A. Margotti[96], A. Marín[86], C. Markert[105], I. Martashvili[112], P. Martinengo[30], M.I. Martínez[1], A. Martínez Davalos[56], G. Martínez García[102], Y. Martynov[2], A. Mas[102], S. Masciocchi[86], M. Masera[26], A. Masoni[93], L. Massacrier[109,102], M. Mastromarco[94], A. Mastroserio[28,30], Z.L. Matthews[91], A. Matyja[102], D. Mayani[55], C. Mayer[104], J. Mazer[112], M.A. Mazzoni[99], F. Meddi[23], A. Menchaca-Rocha[56], J. Mercado Pérez[83], M. Meres[33], Y. Miake[114], A. Michalon[58], L. Milano[26], J. Milosevic[18,ii], A. Mischke[45], A.N. Mishra[82], D. Miśkowiec[86,30], C. Mitu[50], J. Mlynarz[119], A.K. Mohanty[30], B. Mohanty[116], L. Molnar[30], L. Montaño Zetina[8], M. Monteno[95], E. Montes[7], T. Moon[123], M. Morando[22], D.A. Moreira De Godoy[107], S. Moretto[22], A. Morsch[30], V. Muccifora[66], E. Mudnic[103], S. Muhuri[116], H. Müller[30], M.G. Munhoz[107], L. Musa[30], A. Musso[95], B.K. Nandi[41], R. Nania[96], E. Nappi[94], C. Nattrass[112], N.P. Naumov[88], S. Navin[91], T.K. Nayak[116], S. Nazarenko[88], G. Nazarov[88], A. Nedosekin[46], M. Nicassio[28], B.S. Nielsen[72], T. Niida[114], S. Nikolaev[89], V. Nikolic[87], V. Nikulin[76], S. Nikulin[89], B.S. Nilsen[77], M.S. Nilsson[18], F. Noferini[96,9], P. Nomokonov[59], G. Nooren[45], N. Novitzky[38], A. Nyanin[89], A. Nyatha[41], C. Nygaard[72], J. Nystrand[15], A. Ochirov[117], H. Oeschler[53,30], S. Oh[120], S.K. Oh[37], J. Oleniacz[118], C. Oppedisano[95], A. Ortiz Velasquez[55], G. Ortona[30,26], A. Oskarsson[29], P. Ostrowski[118], I. Otterlund[29], J. Otwinowski[86], K. Oyama[83], K. Ozawa[113], Y. Pachmayer[83], M. Pachr[34], F. Padilla[26], P. Pagano[25], G. Paić[55], F. Painke[36], C. Pajares[13], S. Pal[12], S.K. Pal[116], A. Palaha[91], A. Palmeri[97], V. Papikyan[121], G.S. Pappalardo[97], W.J. Park[86], A. Passfeld[54], B. Pastirčák[47], D.I. Patalakha[43], V. Paticchio[94], A. Pavlinov[119], T. Pawlak[118], T. Peitzmann[45], M. Perales[10], E. Pereira De Oliveira Filho[107], D. Peresunko[89], C.E. Pérez Lara[73], E. Perez Lezama[55], D. Perini[30], D. Perrino[28], W. Peryt[118], A. Pesci[96], V. Peskov[30,55], Y. Pestov[3], V. Petráček[34], M. Petran[34], M. Petris[71], P. Petrov[91], M. Petrovici[71], C. Petta[24], S. Piano[98], A. Piccotti[95], M. Pikna[33], P. Pillot[102], O. Pinazza[30], L. Pinsky[110], N. Pitz[52], F. Piuz[30], D.B. Piyarathna[110], M. Płoskoń[68], J. Pluta[118], T. Pocheptsov[59,18], S. Pochybova[60], P.L.M. Podesta-Lerma[106], M.G. Poghosyan[30,26], K. Polák[49], B. Polichtchouk[43], A. Pop[71], S. Porteboeuf-Houssais[64], V. Pospíšil[34], B. Potukuchi[81], S.K. Prasad[119], R. Preghenella[96,9], F. Prino[95], C.A. Pruneau[119], I. Pshenichnov[44], S. Puchagin[88], G. Puddu[21], A. Pulvirenti[24,30], V. Punin[88], M. Putiš[35], J. Putschke[119,120], E. Quercigh[30], H. Qvigstad[18], A. Rachevski[98], A. Rademakers[30], S. Radomski[83], T.S. Räihä[38], J. Rak[38], A. Rakotozafindrabe[12], L. Ramello[27], A. Ramírez Reyes[8], R. Raniwala[82], S. Raniwala[82], S.S. Räsänen[38], B.T. Rascanu[52], D. Rathee[78], K.F. Read[112], J.S. Real[65], K. Redlich[101,57], P. Reichelt[52], M. Reicher[45], R. Renfordt[52], A.R. Reolon[66], A. Reshetin[44], F. Rettig[36], J.-P. Revol[30], K. Reygers[83], L. Riccati[95], R.A. Ricci[67], T. Richert[29], M. Richter[18], P. Riedler[30], W. Riegler[30], F. Riggi[24,97], M. Rodríguez Cahuantzi[1], K. Røed[15], D. Rohr[36], D. Röhrich[15], R. Romita[86], F. Ronchetti[66], P. Rosnet[64], S. Rossegger[30], A. Rossi[22], F. Roukoutakis[79], P. Roy[90], C. Roy[58], A.J. Rubio Montero[7], R. Rui[20], E. Ryabinkin[89], A. Rybicki[104], S. Sadovsky[43], K. Šafařík[30], P.K. Sahu[48], J. Saini[116], H. Sakaguchi[39], S. Sakai[68], D. Sakata[114], C.A. Salgado[13], J. Salzwedel[16], S. Sambyal[81], V. Samsonov[76], X. Sanchez Castro[55,58], L. Šándor[47], A. Sandoval[56], S. Sano[113], M. Sano[114], R. Santo[54], R. Santoro[94,30], J. Sarkamo[38], E. Scapparone[96], F. Scarlassara[22], R.P. Scharenberg[84], C. Schiaua[71], R. Schicker[83], H.R. Schmidt[86,115], C. Schmidt[86], S. Schreiner[30], S. Schuchmann[52], J. Schukraft[30], Y. Schutz[30,102], K. Schwarz[86], K. Schweda[86,83], G. Scioli[19], E. Scomparin[95], R. Scott[112], P.A. Scott[91], G. Segato[22], I. Selyuzhenkov[86], S. Senyukov[27,58], J. Seo[85], S. Serci[21], E. Serradilla[7,56], A. Sevcenco[50], I. Sgura[94], A. Shabetai[102], G. Shabratova[59], R. Shahoyan[30], S. Sharma[81], N. Sharma[78], K. Shigaki[39], M. Shimomura[114], K. Shtejer[6], Y. Sibiriak[89], M. Siciliano[26], E. Sicking[30], S. Siddhanta[93], T. Siemiarczuk[101], D. Silvermyr[75], G. Simonetti[28,30], R. Singaraju[116], R. Singh[81], S. Singha[116], T. Sinha[90], B.C. Sinha[116], B. Sitar[33], M. Sitta[27], T.B. Skaali[18], K. Skjerdal[15], R. Smakal[34], N. Smirnov[120], R. Snellings[45], C. Søgaard[72], R. Soltz[69], H. Son[17], J. Song[85], M. Song[123], C. Soos[30], F. Soramel[22], I. Sputowska[104], M. Spyropoulou-Stassinaki[79], B.K. Srivastava[84], J. Stachel[83], I. Stan[50], I. Stan[50], G. Stefanek[101], G. Stefanini[30], T. Steinbeck[36], M. Steinpreis[16], E. Stenlund[29], G. Steyn[80], D. Stocco[102], M. Stolpovskiy[43], K. Strabykin[88], P. Strmen[33], A.A.P. Suaide[107], M.A. Subieta Vásquez[26], T. Sugitate[39], C. Suire[42], M. Sukhorukov[88], R. Sultanov[46], M. Šumbera[74], T. Susa[87], A. Szanto de Toledo[107], I. Szarka[33], A. Szostak[15], C. Tagridis[79], J. Takahashi[108], J.D. Tapia Takaki[42], A. Tauro[30], G. Tejeda Muñoz[1], A. Telesca[30], C. Terrevoli[28], J. Thäder[86], D. Thomas[45], J.H. Thomas[86], R. Tieulent[109], A.R. Timmins[110], D. Tlusty[34], A. Toia[36,30], H. Torii[39,113], L. Toscano[95], F. Tosello[95], T. Traczyk[118], D. Truesdale[16], W.H. Trzaska[38], T. Tsuji[113], A. Tumkin[88], R. Turrisi[100], T.S. Tveter[18], J. Ulery[52], K. Ullaland[15], J. Ulrich[62,51], A. Uras[109], J. Urbán[35], G.M. Urciuoli[99], G.L. Usai[21],

M. Vajzer[34,74], M. Vala[59,47], L. Valencia Palomo[42], S. Vallero[83], N. van der Kolk[73], P. Vande Vyvre[30], M. van Leeuwen[45], L. Vannucci[67], A. Vargas[1], R. Varma[41], M. Vasileiou[79], A. Vasiliev[89], V. Vechernin[117], M. Veldhoen[45], M. Venaruzzo[20], E. Vercellin[26], S. Vergara[1], D.C. Vernekohl[54], R. Vernet[5], M. Verweij[45], L. Vickovic[103], G. Viesti[22], O. Vikhlyantsev[88], Z. Vilakazi[80], O. Villalobos Baillie[91], L. Vinogradov[117], A. Vinogradov[89], Y. Vinogradov[88], T. Virgili[25], Y.P. Viyogi[116], A. Vodopyanov[59], S. Voloshin[119], K. Voloshin[46], G. Volpe[28,30], B. von Haller[30], D. Vranic[86], G. Øvrebekk[15], J. Vrláková[35], B. Vulpescu[64], A. Vyushin[88], V. Wagner[34], B. Wagner[15], R. Wan[58,40], Y. Wang[83], D. Wang[40], Y. Wang[40], M. Wang[40], K. Watanabe[114], J.P. Wessels[30,54], U. Westerhoff[54], J. Wiechula[115], J. Wikne[18], M. Wilde[54], G. Wilk[101], A. Wilk[54], M.C.S. Williams[96], B. Windelband[83], L. Xaplanteris Karampatsos[105], H. Yang[12], S. Yang[15], S. Yasnopolskiy[89], J. Yi[85], Z. Yin[40], H. Yokoyama[114], I.-K. Yoo[85], J. Yoon[123], W. Yu[52], X. Yuan[40], I. Yushmanov[89], C. Zach[34], C. Zampolli[96,30], S. Zaporozhets[59], A. Zarochentsev[117], P. Závada[49], N. Zaviyalov[88], H. Zbroszczyk[118], P. Zelnicek[30,51], I.S. Zgura[50], M. Zhalov[76], X. Zhang[64,40], Y. Zhou[45], D. Zhou[40], F. Zhou[40], X. Zhu[40], A. Zichichi[19,9], A. Zimmermann[83], G. Zinovjev[2], Y. Zoccarato[109], M. Zynovyev[2]

[1] *Benemérita Universidad Autónoma de Puebla, Puebla, Mexico*
[2] *Bogolyubov Institute for Theoretical Physics, Kiev, Ukraine*
[3] *Budker Institute for Nuclear Physics, Novosibirsk, Russia*
[4] *California Polytechnic State University, San Luis Obispo, CA, United States*
[5] *Centre de Calcul de l'IN2P3, Villeurbanne, France*
[6] *Centro de Aplicaciones Tecnológicas y Desarrollo Nuclear (CEADEN), Havana, Cuba*
[7] *Centro de Investigaciones Energéticas Medioambientales y Tecnológicas (CIEMAT), Madrid, Spain*
[8] *Centro de Investigación y de Estudios Avanzados (CINVESTAV), Mexico City and Mérida, Mexico*
[9] *Centro Fermi – Centro Studi e Ricerche e Museo Storico della Fisica "Enrico Fermi", Rome, Italy*
[10] *Chicago State University, Chicago, IL, United States*
[11] *China Institute of Atomic Energy, Beijing, China*
[12] *Commissariat à l'Energie Atomique, IRFU, Saclay, France*
[13] *Departamento de Física de Partículas and IGFAE, Universidad de Santiago de Compostela, Santiago de Compostela, Spain*
[14] *Department of Physics Aligarh Muslim University, Aligarh, India*
[15] *Department of Physics and Technology, University of Bergen, Bergen, Norway*
[16] *Department of Physics, Ohio State University, Columbus, OH, United States*
[17] *Department of Physics, Sejong University, Seoul, South Korea*
[18] *Department of Physics, University of Oslo, Oslo, Norway*
[19] *Dipartimento di Fisica dell'Università and Sezione INFN, Bologna, Italy*
[20] *Dipartimento di Fisica dell'Università and Sezione INFN, Trieste, Italy*
[21] *Dipartimento di Fisica dell'Università and Sezione INFN, Cagliari, Italy*
[22] *Dipartimento di Fisica dell'Università and Sezione INFN, Padova, Italy*
[23] *Dipartimento di Fisica dell'Università 'La Sapienza' and Sezione INFN, Rome, Italy*
[24] *Dipartimento di Fisica e Astronomia dell'Università and Sezione INFN, Catania, Italy*
[25] *Dipartimento di Fisica 'E.R. Caianiello' dell'Università and Gruppo Collegato INFN, Salerno, Italy*
[26] *Dipartimento di Fisica Sperimentale dell'Università and Sezione INFN, Turin, Italy*
[27] *Dipartimento di Scienze e Tecnologie Avanzate dell'Università del Piemonte Orientale and Gruppo Collegato INFN, Alessandria, Italy*
[28] *Dipartimento Interateneo di Fisica 'M. Merlin' and Sezione INFN, Bari, Italy*
[29] *Division of Experimental High Energy Physics, University of Lund, Lund, Sweden*
[30] *European Organization for Nuclear Research (CERN), Geneva, Switzerland*
[31] *Fachhochschule Köln, Köln, Germany*
[32] *Faculty of Engineering, Bergen University College, Bergen, Norway*
[33] *Faculty of Mathematics, Physics and Informatics, Comenius University, Bratislava, Slovakia*
[34] *Faculty of Nuclear Sciences and Physical Engineering, Czech Technical University in Prague, Prague, Czech Republic*
[35] *Faculty of Science, P.J. Šafárik University, Košice, Slovakia*
[36] *Frankfurt Institute for Advanced Studies, Johann Wolfgang Goethe-Universität Frankfurt, Frankfurt, Germany*
[37] *Gangneung-Wonju National University, Gangneung, South Korea*
[38] *Helsinki Institute of Physics (HIP) and University of Jyväskylä, Jyväskylä, Finland*
[39] *Hiroshima University, Hiroshima, Japan*
[40] *Hua-Zhong Normal University, Wuhan, China*
[41] *Indian Institute of Technology, Mumbai, India*
[42] *Institut de Physique Nucléaire d'Orsay (IPNO), Université Paris-Sud, CNRS-IN2P3, Orsay, France*
[43] *Institute for High Energy Physics, Protvino, Russia*
[44] *Institute for Nuclear Research, Academy of Sciences, Moscow, Russia*
[45] *Nikhef, National Institute for Subatomic Physics and Institute for Subatomic Physics of Utrecht University, Utrecht, Netherlands*
[46] *Institute for Theoretical and Experimental Physics, Moscow, Russia*
[47] *Institute of Experimental Physics, Slovak Academy of Sciences, Košice, Slovakia*
[48] *Institute of Physics, Bhubaneswar, India*
[49] *Institute of Physics, Academy of Sciences of the Czech Republic, Prague, Czech Republic*
[50] *Institute of Space Sciences (ISS), Bucharest, Romania*
[51] *Institut für Informatik, Johann Wolfgang Goethe-Universität Frankfurt, Frankfurt, Germany*
[52] *Institut für Kernphysik, Johann Wolfgang Goethe-Universität Frankfurt, Frankfurt, Germany*
[53] *Institut für Kernphysik, Technische Universität Darmstadt, Darmstadt, Germany*
[54] *Institut für Kernphysik, Westfälische Wilhelms-Universität Münster, Münster, Germany*
[55] *Instituto de Ciencias Nucleares, Universidad Nacional Autónoma de México, Mexico City, Mexico*
[56] *Instituto de Física, Universidad Nacional Autónoma de México, Mexico City, Mexico*
[57] *Institut of Theoretical Physics, University of Wroclaw, Poland*

[58] *Institut Pluridisciplinaire Hubert Curien (IPHC), Université de Strasbourg, CNRS-IN2P3, Strasbourg, France*
[59] *Joint Institute for Nuclear Research (JINR), Dubna, Russia*
[60] *KFKI Research Institute for Particle and Nuclear Physics, Hungarian Academy of Sciences, Budapest, Hungary*
[61] *Kharkiv Institute of Physics and Technology (KIPT), National Academy of Sciences of Ukraine (NASU), Kharkov, Ukraine*
[62] *Kirchhoff-Institut für Physik, Ruprecht-Karls-Universität Heidelberg, Heidelberg, Germany*
[63] *Korea Institute of Science and Technology Information, South Korea*
[64] *Laboratoire de Physique Corpusculaire (LPC), Clermont Université, Université Blaise Pascal, CNRS-IN2P3, Clermont-Ferrand, France*
[65] *Laboratoire de Physique Subatomique et de Cosmologie (LPSC), Université Joseph Fourier, CNRS-IN2P3, Institut Polytechnique de Grenoble, Grenoble, France*
[66] *Laboratori Nazionali di Frascati, INFN, Frascati, Italy*
[67] *Laboratori Nazionali di Legnaro, INFN, Legnaro, Italy*
[68] *Lawrence Berkeley National Laboratory, Berkeley, CA, United States*
[69] *Lawrence Livermore National Laboratory, Livermore, CA, United States*
[70] *Moscow Engineering Physics Institute, Moscow, Russia*
[71] *National Institute for Physics and Nuclear Engineering, Bucharest, Romania*
[72] *Niels Bohr Institute, University of Copenhagen, Copenhagen, Denmark*
[73] *Nikhef, National Institute for Subatomic Physics, Amsterdam, Netherlands*
[74] *Nuclear Physics Institute, Academy of Sciences of the Czech Republic, Řež u Prahy, Czech Republic*
[75] *Oak Ridge National Laboratory, Oak Ridge, TN, United States*
[76] *Petersburg Nuclear Physics Institute, Gatchina, Russia*
[77] *Physics Department, Creighton University, Omaha, NE, United States*
[78] *Physics Department, Panjab University, Chandigarh, India*
[79] *Physics Department, University of Athens, Athens, Greece*
[80] *Physics Department, University of Cape Town, iThemba LABS, Cape Town, South Africa*
[81] *Physics Department, University of Jammu, Jammu, India*
[82] *Physics Department, University of Rajasthan, Jaipur, India*
[83] *Physikalisches Institut, Ruprecht-Karls-Universität Heidelberg, Heidelberg, Germany*
[84] *Purdue University, West Lafayette, IN, United States*
[85] *Pusan National University, Pusan, South Korea*
[86] *Research Division and ExtreMe Matter Institute EMMI, GSI Helmholtzzentrum für Schwerionenforschung, Darmstadt, Germany*
[87] *Rudjer Bošković Institute, Zagreb, Croatia*
[88] *Russian Federal Nuclear Center (VNIIEF), Sarov, Russia*
[89] *Russian Research Centre Kurchatov Institute, Moscow, Russia*
[90] *Saha Institute of Nuclear Physics, Kolkata, India*
[91] *School of Physics and Astronomy, University of Birmingham, Birmingham, United Kingdom*
[92] *Sección Física, Departamento de Ciencias, Pontificia Universidad Católica del Perú, Lima, Peru*
[93] *Sezione INFN, Cagliari, Italy*
[94] *Sezione INFN, Bari, Italy*
[95] *Sezione INFN, Turin, Italy*
[96] *Sezione INFN, Bologna, Italy*
[97] *Sezione INFN, Catania, Italy*
[98] *Sezione INFN, Trieste, Italy*
[99] *Sezione INFN, Rome, Italy*
[100] *Sezione INFN, Padova, Italy*
[101] *Soltan Institute for Nuclear Studies, Warsaw, Poland*
[102] *SUBATECH, Ecole des Mines de Nantes, Université de Nantes, CNRS-IN2P3, Nantes, France*
[103] *Technical University of Split FESB, Split, Croatia*
[104] *The Henryk Niewodniczanski Institute of Nuclear Physics, Polish Academy of Sciences, Cracow, Poland*
[105] *The University of Texas at Austin, Physics Department, Austin, TX, United States*
[106] *Universidad Autónoma de Sinaloa, Culiacán, Mexico*
[107] *Universidade de São Paulo (USP), São Paulo, Brazil*
[108] *Universidade Estadual de Campinas (UNICAMP), Campinas, Brazil*
[109] *Université de Lyon, Université Lyon 1, CNRS/IN2P3, IPN-Lyon, Villeurbanne, France*
[110] *University of Houston, Houston, TX, United States*
[111] *University of Technology and Austrian Academy of Sciences, Vienna, Austria*
[112] *University of Tennessee, Knoxville, TN, United States*
[113] *University of Tokyo, Tokyo, Japan*
[114] *University of Tsukuba, Tsukuba, Japan*
[115] *Eberhard Karls Universität Tübingen, Tübingen, Germany*
[116] *Variable Energy Cyclotron Centre, Kolkata, India*
[117] *V. Fock Institute for Physics, St. Petersburg State University, St. Petersburg, Russia*
[118] *Warsaw University of Technology, Warsaw, Poland*
[119] *Wayne State University, Detroit, MI, United States*
[120] *Yale University, New Haven, CT, United States*
[121] *Yerevan Physics Institute, Yerevan, Armenia*
[122] *Yildiz Technical University, Istanbul, Turkey*
[123] *Yonsei University, Seoul, South Korea*
[124] *Zentrum für Technologietransfer und Telekommunikation (ZTT), Fachhochschule Worms, Worms, Germany*

[*] Corresponding author.
E-mail address: nicole.bastid@clermont.in2p3.fr (N. Bastid).

[i] Also at: M.V. Lomonosov Moscow State University, D.V. Skobeltsyn Institute of Nuclear Physics, Moscow, Russia.

[ii] Also at: “Vinča” Institute of Nuclear Sciences, Belgrade, Serbia.